

# Prediction of Large-Scale Wildfires With the Canopy Stress Index Derived from Soil Moisture Active Passive

Lee Ju Hyoung<sup>✉</sup>

**Abstract**—Land surface variables such as surface soil moisture are recognized as important wildfire indicators. However, quantifying wildfire fuel combustibility through only satellite-retrieved soil moisture remains challenging, because soil moisture does not provide information about vegetation (fuel) moisture and water availability to plants is complicated by another factor of soil properties. Thus, to enhance the wildfire prediction ability of the soil moisture active passive (SMAP) mission, this study examines a canopy stress index (CSI) retrieved from 1 km SMAP level 2 products. The strong relationship between prefire CSI and fire severity is demonstrated over two large-scale (greater than 1000 ha) wildfires in Gang-won Province, South Korea. CSI can effectively predict the severity of large-scale wildfires one week before fire events, differentiating dry soils from wildfire hazards. SMAP L2 data with a temporal resolution of 5–7 d over the study sites are suitable for supporting aerial firefighting activities and reducing false fire warnings.

**Index Terms**—Canopy stress index (CSI), canopy temperature, large-scale wildfire prediction, soil moisture active passive (SMAP) brightness temperature.

## I. INTRODUCTION

WILDFIRES, out-of-control fires in areas with “combustible vegetation” [1], are becoming increasingly frequent and larger in scale worldwide. They result in unexpected catastrophes, such as economic losses, causalities, and losses of natural resources.

According to the US Forest Service, more than 7860 wildfires occurred in California, in 2019 and burned 105 147 ha. Suppression efforts cost as much as 163 million dollars. According to Alberta Wildfire in Canada, 1005 wildfires occurred in Alberta, in 2019, and burned 883 413.70 ha. In the Amazon, more than 40 000 wildfires burned 906 000 ha, in 2019. These fires have common traits, and the burned areas are increasing according to several reports from the US National Climate Assessment, European Environment Agency, and National Forestry Database of Canada. This increasing fire occurrence and severity are not

Manuscript received March 18, 2020; revised December 14, 2020; accepted December 23, 2020. Date of publication December 29, 2020; date of current version February 3, 2021. This work was supported in part by the National Research Foundation of the Korean Government under Grant NRF-2018R1D1A1B07048817. (*Corresponding author: Lee Ju Hyoung.*)

The author is with the Future and Fusion Lab of Architectural, Civil and Environmental Engineering, Korea University, Seoul 02841, South Korea (e-mail: ju.lee@mail.com).

Digital Object Identifier 10.1109/JSTARS.2020.3048067

unrelated to anthropogenic causes such as increasing population density, the development of extensive wildland urban interface areas, excessive forestry management (i.e., overgrowth), or human activity in line with climate change such as drought and heatwaves [2], [3]. Accordingly, there is an increasing need to establish wildfire risk prediction systems.

Most current fire prediction models usually consider meteorological factor-based drought conditions such as the Palmer Drought Severity Index, which mainly consists of monthly temperature and precipitation anomalies. However, they neglect the key factor of the fuel moisture of combustible biomass [2]–[5]. Additionally, in terms of time scale, wildfire documentation usually focuses on monthly trends or historical records of postfire-related climatological variations, rather than on early warning or urgent action through real time monitoring [1]. Thus, monitoring of prefire fuel moisture conditions is often lacking.

Currently, satellite-retrieved fire products do not forewarn of the hazards before fire occurrence. Moderate resolution imaging spectroradiometer (MODIS) data are widely used, but they are postfire products such as burned area and active fire products [6]. Sentinel-2 multispectral instrument (MSI) reflectance measurements and Sentinel-1 backscattering are often applied. However, they also estimate the burned area after the occurrence of fires [7], [8]. Laneve and Cadau [9] have demonstrated that the spinning enhanced visible and infrared imager sensor on the satellite Meteosat Second Generation is suitable for early detection, but only for small-scale fire events (less than 4 km). Fire area or temperature have been found to be overestimated by less than 20%. In addition, because of a short prediction range, responses are possible only when field guards actually observe the fire events with their eyes. Parto *et al.* [10] have also attempted to make an early detection based on MODIS brightness temperature. However, this method was also developed for small-scale fires. It is not supportive of aerial firefighting over large scale.

No previous studies have aimed at early warning or prediction of large-scale wildfires or the reduction of fire hazards before disasters. For large-scale fires, the quantitative comparison of spatial distribution is important, unlike small-scale fires. Recently, satellite-retrieved surface soil moisture has been used to assess wildfires across ecosystems, owing to its close relationship with fire occurrence [1], [11], [12]. However, in fact, SMAP soil moisture detects soil emission beneath vegetation. Wildfires largely depend on the vegetation moisture and type, rather than

on the soil itself. If there is no biomass to burn, no fire occurs, even in extremely dry soils. Thus, using only satellite-retrieved soil moisture is likely to generate false warnings.

Hence, to take the combustibility of vegetation into account, fuel moisture information, such as the dryness of trees or the leaves fallen on the land surface, should be included in fire prediction. Canopy temperature can be used as a proxy for fuel moisture of vegetation, although it has been previously suggested to estimate crop yield and water requirement [13]. The method to estimate canopy temperature with remotely sensed brightness temperature has been well developed for infrared radiometers [14], [15]. This study applies this approach to SMAP/Sentinel-1 L2 Radiometer/Radar EASE-Grid Soil Moisture data, thus advancing remote sensing-based fire prediction capabilities. Compared with infrared radiometers, L-band microwave SMAP instruments are independent of cloud cover and can provide both night and day measurements [17].

For timely and prompt fire suppression, this study suggests use of the canopy stress index (CSI) retrieved from 1 km SMAP L2 products, on the basis of the rationale that the energy state prereads the combustibility of biomass leading to wildfires later. Because it indicates the moisture of vegetation as combustible fuel, the index is more specific for wildfire prevention than the SMAP surface soil moisture product. In addition, it reports the fuel combustibility specifically at the time of satellite detection instead of monthly or yearly climatology. The objective of this study is to illustrate a positive relationship between prefire CSI and fire severity and to evaluate whether the SMAP products with a temporal resolution of 5–7 d are sufficient for a timely prediction of large-scale wildfires.

## II. MATERIALS AND METHODS

### A. Study Area

Two large-scale fire events with more than 1000 ha of burned area occurred in the Republic of Korea, in 2019. These mountainous areas are covered mostly by needle leaf trees (forestry spatial information provided by the Korean government, Forest Geospatial Information System (FGIS).<sup>1</sup> Go-sung is located at longitude 128°30' to 128°35' and latitude 38°12' to 38°15'. On April 4th, outbreak of wildfires occurred at this location. The burned area (1757 ha) is indicated in Fig. 1 in red. The wildfire was presumed to have been ignited in the night by electric spikes and to have rapidly spread through the forests to the city, owing to strong wind and dry air. According to the central disaster safety headquarters of the Korean government, the conditions were dry and windy (wind speed of 5–26 m/s, humidity of 10–30%, and air temperature of 10.8 °C) at the time of the fire events. The monthly precipitation is 68.7 mm, in April. The soil texture is sandy loam.<sup>2</sup> On the same day, another large-scale wildfire occurred nearby in Gang-neung at longitude 129° to 129°5' and latitude 37°34' to 37°37'. This area is surrounded by Gang-neung city in Gang-won province. The burned area was approximately 1260 ha, as shown in Fig. 1. The meteorological conditions are similar to those at Go-sung. However, the land use is slightly

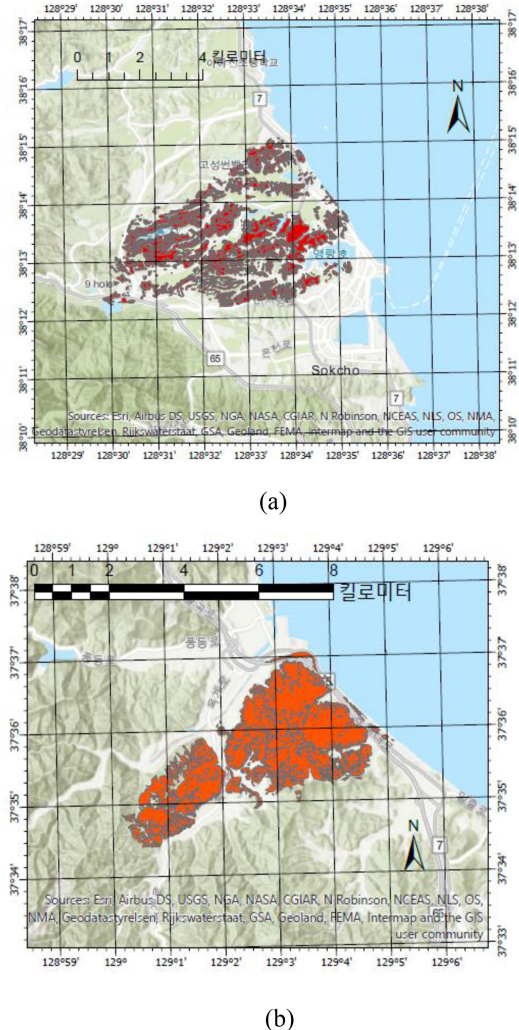


Fig. 1. Two fire events in Go-sung (left) and Gang-neung (right) in Gang-won province are shown in red.

TABLE I  
LAND SURFACE CONDITIONS AND FIRE SEVERITY

	Gosung	Gangneung
<b>Forest type</b>	mixed forest	mixed forest
<b>Land cover</b>	forest, arable land, urban, resort area	forest
<b>Burned area</b>	1757 ha	1260 ha
<b>Suppression time</b>	23 hours	22 hours

more diverse, including arable land, fruit trees, grassland, and forests. The two fire areas are compared in Table I.

### B. SMAP Data

The NASA soil moisture active passive (SMAP) mission is equipped with an L-band radiometer, which measures the brightness temperature to determine the surface soil moisture from the

<sup>1</sup>[Online]. Available: <http://www.forest.go.kr>

<sup>2</sup>[Online]. Available: <https://soil.rda.go.kr/soil/soilmapper/crop.jsp>

top  $\sim 5$  cm of soil. It has an intermediate spatial resolution of  $\sim 9$  km and records twice (ascending and descending) per day [16]. For 1 km SMAP brightness temperature and surface soil moisture, L2 SMAP\_L2\_SM\_SP\_1AIWDV data (ver. 2) were acquired from EOSDIS earth data [17]. In addition, the leaf area index (LAI) data required to calculate canopy temperature were from 500 m MCD15A3H C6 products from Terra MODIS (Myneni *et al.*, 2015).

### C. Canopy Temperature

At L-band frequencies, atmospheric transmissivity is almost 1, and SMAP brightness temperature products are atmospherically corrected (Entekhabi *et al.*, 2014). When SMAP measures brightness temperature, the emission from both the soil and overlaying canopy is considered. In the presence of sparsely distributed vegetation, SMAP signal is considered to be transmitted from the underlying soil. However, owing to an absorbing layer of vegetation, the SMAP brightness temperature over forest area or dense vegetation layer is primarily observed from vegetation than soil [18]. Thus, this limitation of SMAP soil moisture retrieval algorithm becomes a merit for detecting the forest area.

The canopy temperature is estimated from this brightness temperature. In more detail, the directional radiometric surface temperature  $T_R$  is estimated from the SMAP brightness temperature measurement  $T_B$  at view angle  $\theta$  and directional thermal emissivity  $\varepsilon$  [19].

$$T_R(\theta) = \{[T_B(\theta)^n - (1 - \varepsilon(\theta))T_{\text{sky}}^n]/\varepsilon(\theta)\}^{1/n} \quad (1)$$

where  $n$ , the power in the Stefan-Boltzman equation is calculated for the L-band wavelength (21 cm) and temperature range from 190 to 315 K [14], and the hemispherical temperature of the sky  $T_{\text{sky}}$  is 2.7 K [15].  $T_R$  is further used to calculate the canopy temperature  $T_C$

$$T_C = \{[T_R(\theta)^n - (1 - f)T_s^n]/f\}^{1/n} \quad (2)$$

where  $T_s$  is the soil surface temperature, and  $f$  is the canopy fraction as a function of the LAI [19]. For vegetation in this study site, the LAI is multiplied by a clumping factor of 0.8 [20].

Quantitative comparison of the land surface variables detected by remote sensors with other variables or those in other surface conditions is difficult because the land surface is highly heterogeneous and complicated by several other associated factors such as soil texture, soil property, or vegetation. Thus, additional information is needed. If two moisture indicators for the soil as well as the canopy are both consistent, then the combined index indicates the surface state more clearly. Thus, (3) is expressed as a ratio of two variables. The proposed CSI is as follows:

$$\text{CSI} = \frac{T_C[K]}{\text{SMAP surface soil moisture [%]}}. \quad (3)$$

Because of limited SMAP data availability over study sites, there is a time gap. For Go-sung, the prefire CSI is set on March 28th, whereas the postfire CSI is on April 8th. For Gang-neung, the prefire CSI is estimated with SMAP data acquired on March 28th, whereas SMAP data on April 15th are used for the postfire CSI.

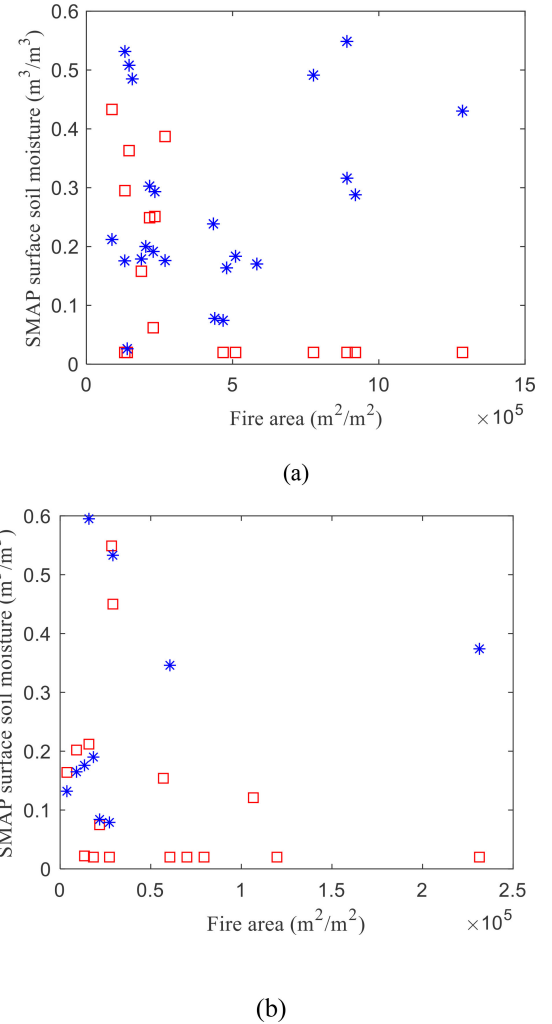


Fig. 2. SMAP soil moisture over the fire area before (□) and after (\*) the fire events. (a) Gang-neung. (b) Go-sung.

## III. RESULTS AND DISCUSSION

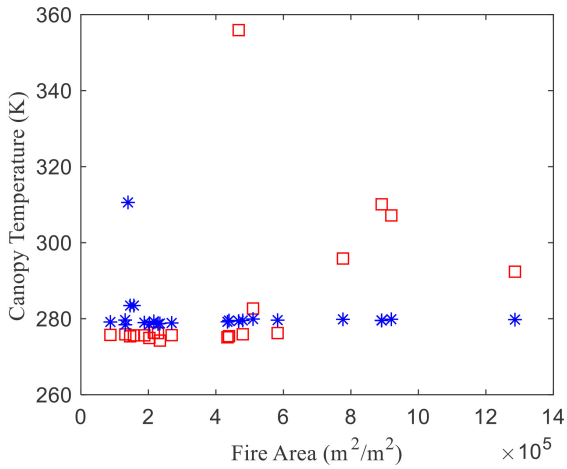
Among potential wildfire predictors, the three indicators shown below (SMAP soil moisture, canopy temperature, and CSI) are associated with fire severity, rather than root zone soil moisture or vegetation water content (data not shown).

### A. SMAP Surface Soil Moisture

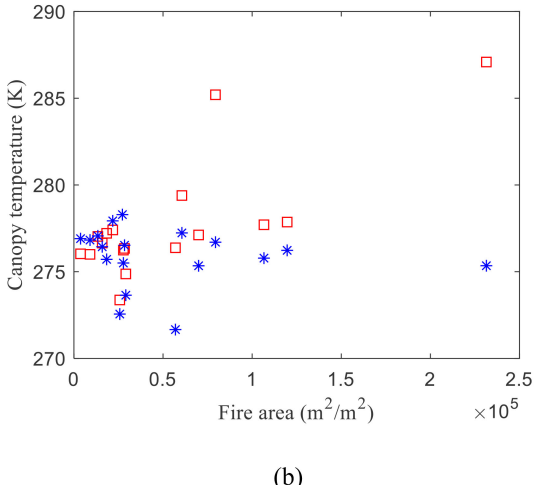
The prefire surface soil moisture is, in some degree, related to wildfire combustibility. Fig. 2 shows the SMAP surface soil moisture over the fire area before and after the fires. The SMAP surface soil moisture is very low on March 28th, before the fires. Interestingly, this dry soil area is proportional to the fire severity in the fire area. At both sites in Go-sung and Gang-Neung, the larger the burned area, the drier the soil. Thus, the spatial distribution of low soil moisture may be important for assessing large-scale wildfire risk. In Table II, a spatial average of the prefire soil moisture in Go-sung is low at  $0.13 \text{ m}^3/\text{m}^3$ , whereas it recovered to moderate levels at  $0.267 \text{ m}^3/\text{m}^3$  after the fire. Similarly, Gang-neung was very dry at  $0.147 \text{ m}^3/\text{m}^3$  before the

TABLE II  
SPATIAL AVERAGE OF LAND SURFACE VARIABLES OVER BURNED AREAS

	GO-SUNG		GANG-NEUNG	
	Before the fire event	After the fire event	Before the fire event	After the fire event
Soil moisture ( $\text{m}^3/\text{m}^3$ )	0.13	0.267	0.147	0.272
Brightness temperature (K)	258.6	238.3	262.3	258.4
Canopy temperature (K)	281.8	275.9	293.9	281
CSI (K%)	79.7	16.15	88.6	17.9



(a)



(b)

Fig. 3. Canopy temperature over fire areas before (□) and after (\*) fire events. (a) Gang-neung. (b) Go-sung.

fire event, thus suggesting that surface heat gradually accumulates. However, soil moisture was resilient, and recovered to moderate levels at  $0.272 \text{ m}^3/\text{m}^3$  after the fire event. This result is in agreement with previous findings that surface soil moisture is indicative of fire occurrence [1], [11].

#### B. Canopy Temperature

In Fig. 3, elevated prefire canopy temperatures at both sites are quenched after the fire events. That is, the higher the canopy

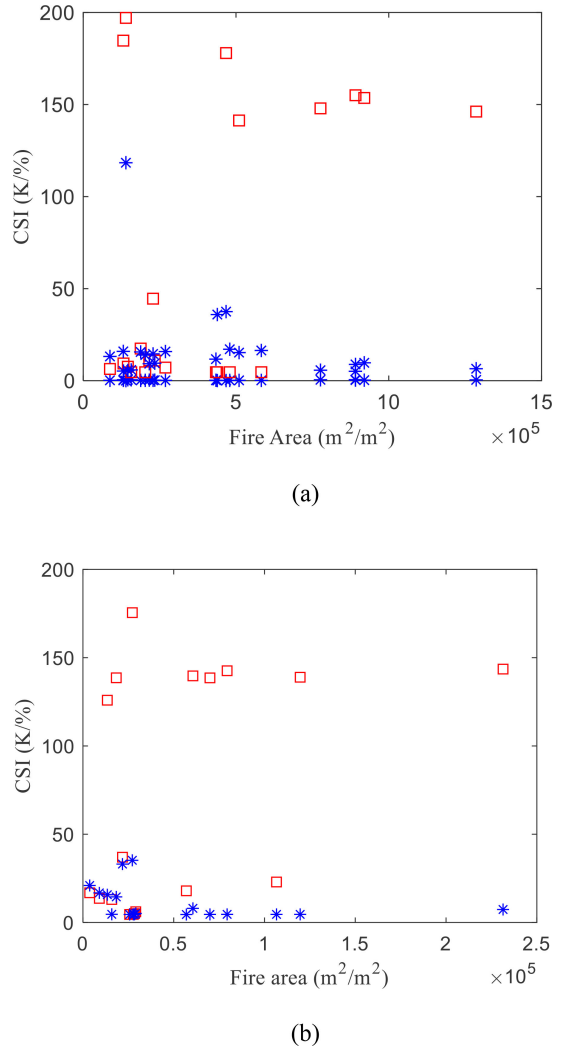


Fig. 4. CSI over the fire area before (□) and after (\*) fire events. (a) Gang-neung. (b) Go-sung.

temperature, the more vulnerable to fire outbreak the area. High canopy temperature indirectly indicates lower fuel moisture, thus suggesting that a forest is combustible, and the fire is ready to easily propagate. As shown in (1), high brightness temperature contributes to high canopy temperature. More specifically, as shown in Table II, the prefire brightness temperature in Go-sung is higher (by approximately 20 K) than the postfire levels. The prefire brightness temperature in Gang-neung is higher (by approximately 4 K) than the postfire levels. The change in the brightness temperature is thus important for monitoring fuel moisture [9], [10].

#### C. Canopy Stress Index

Assessing vegetation dryness (fuel moisture) or combustibility across locations is difficult by simply examining only the surface soil moisture or only canopy temperature. For example, in Table II, the brightness temperature in Go-sung decreases from 258.6 to 238.3 K after the fire, whereas it decreases from 262.3 to 258.4 K in Gang-neung after the fire. It is noteworthy that the postfire brightness temperature in Gan-neung is similar

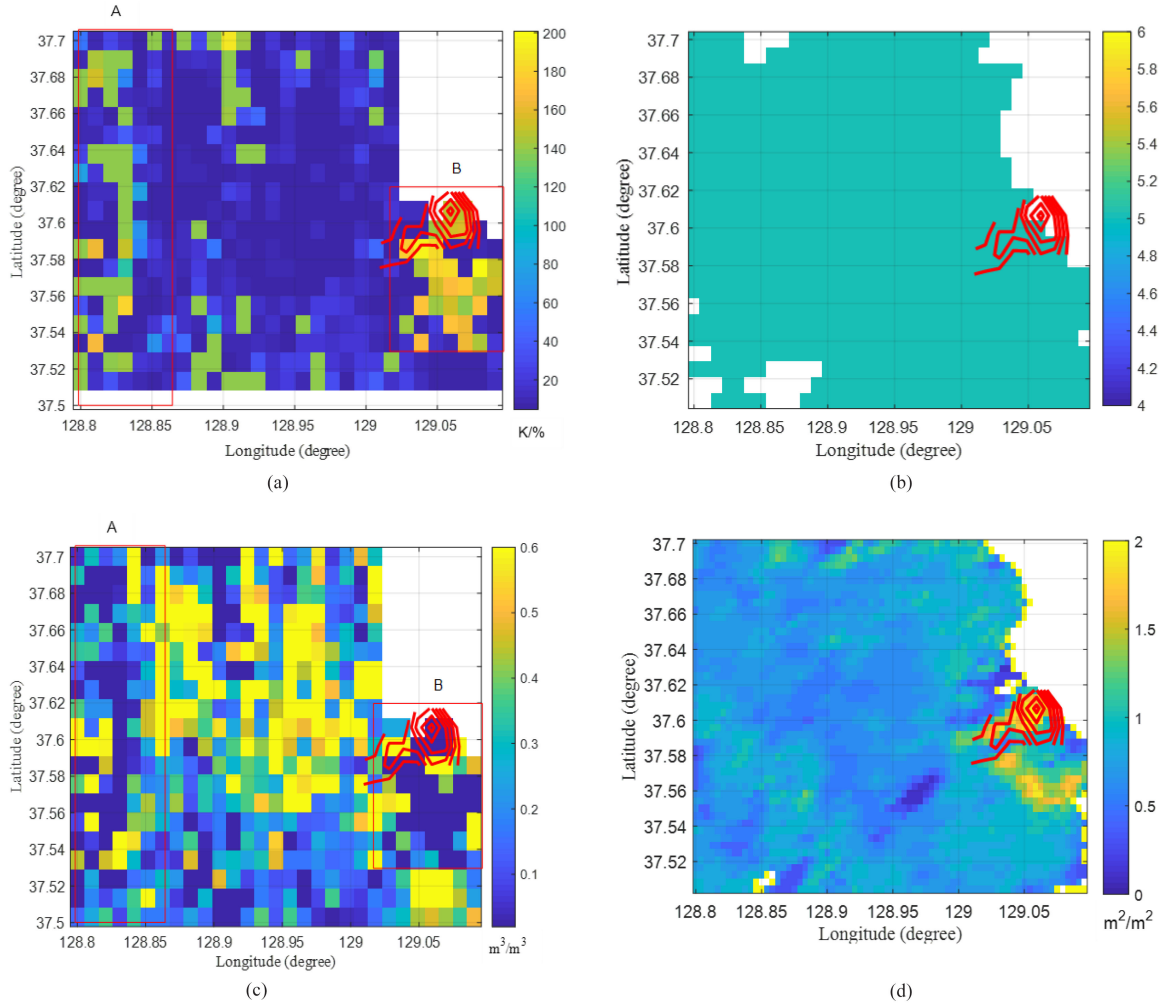


Fig. 5. Spatial distribution at Gang-neung one week before the fire events. (a) CSI. (b) MODIS active fire (5: no-fire land). (c) SMAP soil moisture. (d) LAI. Ocean is shown by white pixels, whereas fire area is shown by red contours.

to the prefire brightness temperature in Go-sung. Thus, only brightness temperature does not allow to discriminate the prefire states from the postfire. Soil moisture also has the similar nature. For example, 15% of soil moisture has available water to plants in sandy loam, but not in clay. Thus, a direct comparison of the fuel moisture state between locations is often difficult, owing to the complications of the weather, soil texture, vegetation, and climatic factors [21].

In contrast, the CSI is a canopy moisture index normalized to soil moisture. Despite heterogeneity in land surface conditions, the CSI at one location can be compared with the CSI at a different location under different soil and vegetation moisture conditions. More specifically, in Table II, the spatially averaged prefire CSI is higher, at approximately 80–90 K/% (before averaging, its range is 150–200 K/%), at both sites. However, the postfire CSI is lower, at 16–18 K/%, at both sites. Further comparison is graphically illustrated in Fig. 4, in which the prefire CSI is much higher than the postfire CSI. At both sites, the higher the CSI, the greater the fire severity. As compared with surface soil moisture in Fig. 2 or canopy temperature in Fig. 3, the CSI is more effective for differentiating between

prefire and postfire events. In addition, as compared with existing meteorological parameters used by fire prediction models, such as humidity or air temperature [5], the CSI is a more direct indicator of fuel moisture.

Fig. 5 further compares the spatial distribution of CSI, SMAP, and MODIS active fire data over the Gang-neung site. The CSI appropriately predicts fire risk at high values around 150–200 K/% 1 week before the fire events. In Fig. 5(a), the fire is shown by red contours, whereas the CSI prediction is shown in yellow pixels. When the CSI does not provide a warning of wildfire over box A, fire did not occur. However, surface soil moisture gives a false warning over box A in Fig. 5(c). In box B, fire actually occurred, when CSI appropriately gives a warning. However, this fire occurrence is not detected by MODIS active fire data captured during the fire burning period (March 28th–April 6th), as shown in Fig. 5(b) (5 implies no fire land). As discussed above, in Fig. 5(c), the SMAP soil moisture overestimates the fire risk, producing false warnings about all the dry soils in both box A (in which no fire occurred) and B (in which fire occurred). In Fig. 5(d), although the forest area is appropriately located by

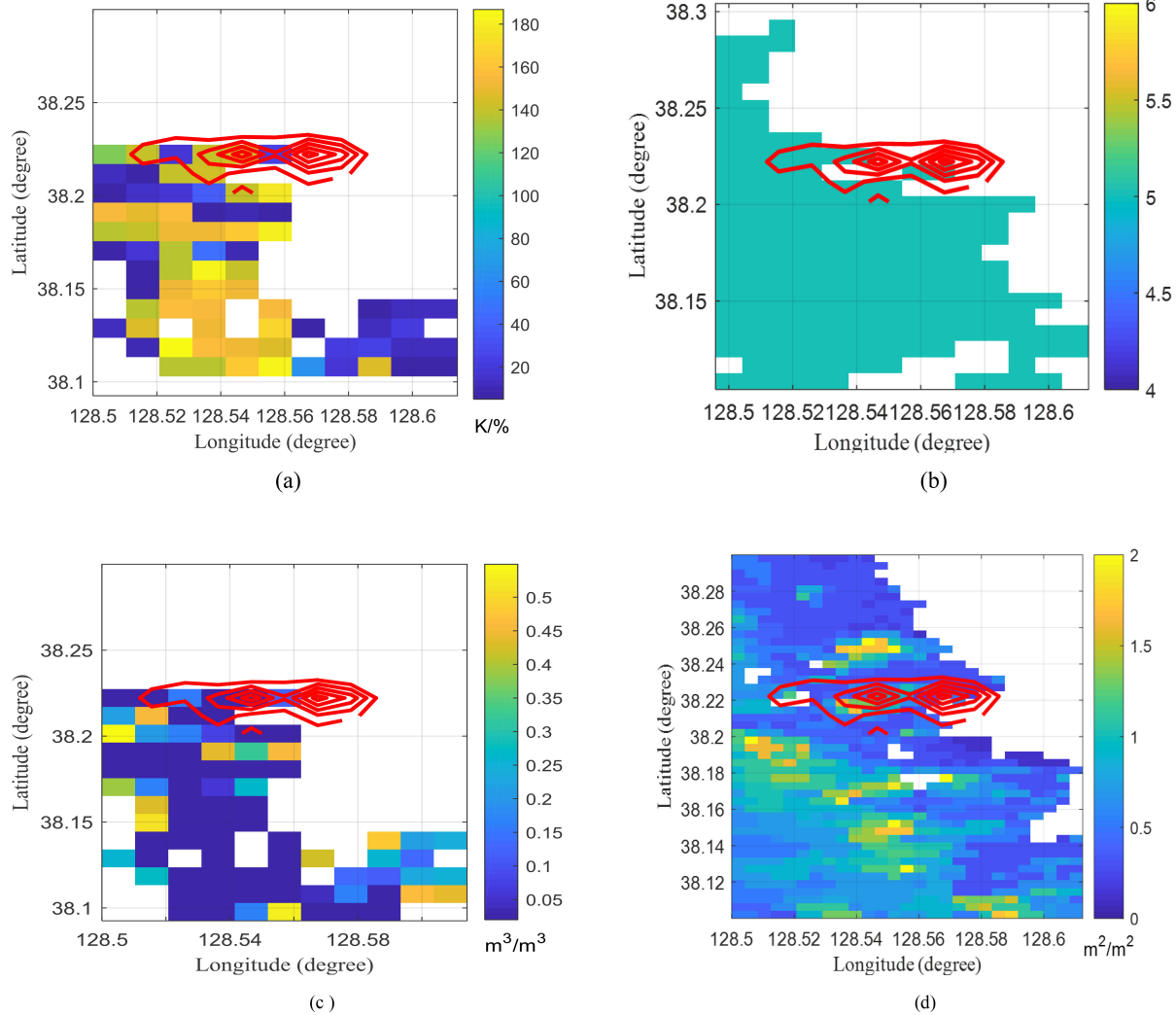


Fig. 6. Spatial distribution at Go-Sung one week before the fire events. (a) CSI. (b) MODIS active fire (5: no-fire land). (c) SMAP soil moisture. (d) LAI. Ocean and urban areas are masked by white pixels, whereas fire area is shown by red contours.

the LAI, their fuel moisture information is unknowable with the LAI only.

The same approach is also applied to the other fire event in Go-sung. Fire risk is appropriately predicted by the CSI. In Fig. 6(a), fire occurs in high CSI pixels at 150 K/% around 38.22° latitude. However, unlike that at Gang-neung, the fire area in the red contour also includes several low CSI pixels in blue and white, where white pixels indicate the unavailability of SMAP data, and blue pixels aggregate nonfire areas at higher resolution. The fire area in this location is sparsely distributed, and the fire area size is also smaller than that at Gang-neung, as shown in Fig. 4 (the maximum fire area at Go-sung is  $2 \times 10^5 \text{ m}^2/\text{m}^2$ , whereas that at Gang-neung is approximately  $13 \times 10^5 \text{ m}^2/\text{m}^2$ ).

In Fig. 6(a), other high CSI pixels (at 38.1–38.15° latitude), in yellow, located below the fire area are also suggested to have high fire risk, meaning that wildfires could have spread more widely than actually occurred in the red contour area. In particular, this mountainous region in yellow is covered with deciduous trees according to FGIS forestry spatial information. These trees are all considered combustible. However, at the same time, we

cannot exclude the possibility that the high CSI pixels in yellow might be overestimated because of the sensitivity of LAI data to certain vegetation type. Previously, the LAI has been found to tend to overestimate deciduous trees, owing to clumping, scale effects, or vegetation density [22]–[25]. If the vegetation index, such as the normalized difference vegetation index or LAI, is overestimated, then the canopy temperature and CSI may also be overestimated through (2) and (3). Thus, to mitigate any possible biases arising from a selection of input data, use of CSI along with forestry information is recommended.

In Fig. 6(b), the MODIS active fire data captured during the fire burning period (March 28th–April 6th) do not indicate fire events. In Fig. 6(c), the SMAP soil moisture is similar to the CSI in Fig. 6(a). However, the fire risk in dry soils at the longitude of 128.56°–128.59° appears to be overestimated relative to the CSI. In Fig. 6(d), the distribution of vegetation is detected with the LAI, but the moisture as fuel combustibility is not indicated.

Overall, the CSI is suggested as a fire-risk index over large-scale area. It can be used to develop urgent fire suppression strategies one week before a fire outbreak. For example, for

aerial firefighting, tactical aircrafts may direct air tankers and helicopters to high CSI areas. Safety measures may include early warnings, restriction of trespassing, examination of electric transformers, spreading fire retardants or water with aircrafts, or removal of fallen leaves over the fire-risk area beforehand.

#### IV. CONCLUSION

Two recent wildfires in Kang-won province are characterized by extreme events with high damage but low frequency. In this study, a novel index, the CSI, is suggested to support aerial firefighting over large-scale fire disasters one week beforehand. By including vegetation moisture, as an indirect indicator of fire fuel moisture, this index covers the missing piece in existing fire management scheme, which considers only meteorological parameters, (e.g., wind, humidity, and air temperature) and forestry information. In addition, an SMAP L2 temporal resolution of 5–7 d over the study area is considered sufficient for fire prevention with this index.

A merit of the CSI is that it is a standardized index. Because of the high surface heterogeneity, the canopy temperature values indicating fire risk in a certain location do not predict fire occurrence in other areas. **Soil moisture alone does not accurately inform about fuel moisture, because water availability to plants is dependent on another factor of soil property.** However, a quantitative comparison with CSI is possible. When broadly applied across locations, a CSI at 150–200 K/% indicates high wildfire risk, whereas 10–20 K/% implies low risk. Thus, the CSI can be used as a large-scale index.

For establishing fire prevention plans with tactical aircrafts, future studies may further assess the capability of this index to serve as a large-scale fire predictor. Because the main features of climate change-driven disasters are uncontrollability and overwhelmingly large burning area size, the CSI may be combined with weather information to assess how rapidly the fire may propagate, and in which direction it may spread.

#### REFERENCES

- [1] D. Jensen, J. T. Reager, B. Zajic, N. Rousseau, M. Rodell, and E. Hinkley, “The sensitivity of US wildfire occurrence to pre-season soil moisture conditions across ecosystems,” *Environ. Res. Lett.*, vol. 13, no. 1, Jan. 2018, Art. no. 014021.
- [2] J. San-Miguel-Ayanz, J. M. Moreno, and A. Camia, “Analysis of large fires in European Mediterranean landscapes: Lessons learned and perspectives,” *Forest Ecol. Manage.*, vol. 294, pp. 11–22, Apr. 2013.
- [3] F. Tedim, G. Xanthopoulos, and V. Leone, “Forest fires in Europe: Facts and challenges,” in *Wildfire Hazards, Risks and Disasters*, J. F. Shroder and D. Paton, Eds., Oxford, U.K.: Elsevier, 2015, ch. 5, pp. 77–99.
- [4] D. A. Peterson *et al.*, “The 2013 Rim fire: Implications for predicting extreme fire spread, pyroconvection, and smoke emissions,” *Bull. Amer. Meteorological Soc.*, vol. 96, no. 2, pp. 229–247, Feb. 2014.
- [5] B.D. Amiro *et al.*, “Fire weather index system components of large fires in the Canadian boreal forest,” *Int. J. Wildland Fire*, vol. 13, pp. 391–400, Jan. 2004.
- [6] D. P. Roy, L. Boschetti, C. O. Justice, and J. Ju, “The collection 5 MODIS burned area product—Global evaluation by comparison with the MODIS active fire product,” *Remote Sens. Environ.*, vol. 112, no. 9, pp. 3690–3707, Sep. 2008.
- [7] E. Roteta, A. Bastarrika, M. Padilla, T. Storm, and E. Chuvieco, “Development of a Sentinel-2 burned area algorithm: Generation of a small fire database for sub-Saharan Africa,” *Remote Sens. Environ.*, vol. 222, pp. 1–17, Mar. 2019.
- [8] M. Belenguer-Plomer, E. Chuvieco, and M. Tanase, “Sentinel-1 based algorithm to detect burned areas,” in *Proc. 11th EARSeL Forest Fires SIG Workshop*, 2017, pp. 1–13.
- [9] G. Laneve and E. Cadau, “Performances assessment of the SFIDE algorithm devoted to early fire detection by using SEVIRI/MSG images,” in *Proc. 4th Wildfire Conf.*, Siviglia, Spagna, May 2007. [Online]. Available: [https://www.researchgate.net/publication/228878776\\_Performances\\_assessment\\_of\\_the\\_SFIDE\\_algorithm\\_devoted\\_to\\_early\\_fire\\_detection\\_by\\_using\\_SEVIRIMSG\\_images](https://www.researchgate.net/publication/228878776_Performances_assessment_of_the_SFIDE_algorithm_devoted_to_early_fire_detection_by_using_SEVIRIMSG_images)
- [10] F. Parto, M. Saradjian, and S. Homayouni, “MODIS brightness temperature change-based forest fire monitoring,” *J. Indian Soc. Remote Sens.*, vol. 48, no. 1, pp. 163–169, Jan. 2020.
- [11] E. S. Krueger, T. E. Ochsner, D. M. Engle, J. D. Carlson, D. Twidwell, and S. D. Fuhlendorf, “Soil moisture affects growing-season wildfire size in the southern great plains,” in English, *Soil Sci. Soc. America J.*, vol. 79, pp. 1567–1576, 2015.
- [12] N. C. Dadap, A. R. Cobb, A. M. Hoyt, C. F. Harvey, and A. G. Konings, “Satellite soil moisture observations predict burned area in Southeast Asian peatlands,” *Environ. Res. Lett.*, vol. 14, no. 9, Sep. 2019, Art. no. 094014.
- [13] R. D. Jackson, S. Idso, R. J. Reginato, and P. Pinter, “Canopy temperature as a crop water stress indicator,” *Water Resour. Res.*, vol. 17, Apr. 1981.
- [14] F. Becker and Z.-L. Li, “Temperature-independent spectral indices in thermal infrared bands,” *Remote Sens. Environ.*, vol. 32, no. 1, pp. 17–33, Apr. 1990.
- [15] T. R. H. Holmes, W. T. Crow, C. Hain, M. C. Anderson, and W. P. Kustas, “Diurnal temperature cycle as observed by thermal infrared and microwave radiometers,” *Remote Sens. Environ.*, vol. 158, pp. 110–125, Mar. 2015.
- [16] C. Cui *et al.*, “Soil moisture mapping from satellites: An intercomparison of SMAP, SMOS, FY3B, AMSR2, and ESA CCI over two dense network regions at different spatial scales,” *Remote Sens.*, vol. 10, no. 1, 2018.
- [17] N. Das *et al.*, *SMAP/Sentinel-1 L2 Radiometer/Radar 30-Second Scene 3 km EASE-Grid Soil Moisture*, Version 2. Boulder, CO, USA: NASA National Snow and Ice Data Center Distributed Active Archive Center, 2018. doi: [10.5067/KE1CSVXMI95Y](https://doi.org/10.5067/KE1CSVXMI95Y).
- [18] D. Chaparro, M. Piles, M. Vall-llossera, A. Camps, A. G. Konings, and D. Entekhabi, “L-band vegetation optical depth seasonal metrics for crop yield assessment,” *Remote Sens. Environ.*, vol. 212, pp. 249–259, Jun. 2018.
- [19] W. P. Kustas and J. M. Norman, “A two-source approach for estimating turbulent fluxes using multiple angle thermal infrared observations,” *Water Resour. Res.*, vol. 33, no. 6, pp. 1495–1508, Jun. 1997.
- [20] J.-M. N. Walter, R. Fournier, K. Soudani, E. Meyer, and J. M. N. Walter, “Integrating clumping effects in forest canopy structure: An assessment through hemispherical photographs,” *J. Remote Sens.*, vol. 29, pp. 388–410, Jun. 2003.
- [21] N. Zhang, S. M. Quiring, and T. W. Ford, “Blending SMAP, Noah and in situ soil moisture using multiple methods,” *Hydrol. Earth Syst. Sci. Discuss.*, 2019, pp. 1–50.
- [22] B. Xu *et al.*, “Analysis of global LAI/FPAR products from VIIRS and MODIS sensors for spatio-temporal consistency and uncertainty from 2012–2016,” *Forests*, vol. 9, no. 2, pp. 1–21, 2018.
- [23] K. Yan *et al.*, “Evaluation of MODIS LAI/FPAR product collection 6. Part 1: Consistency and improvements,” *Remote Sens.*, vol. 8, no. 5, pp. 1–16, 2016.
- [24] K. Yan *et al.*, “Evaluation of MODIS LAI/FPAR product collection 6. Part 2: Validation and intercomparison,” *Remote Sens.*, vol. 8, no. 6, pp. 1–26, 2016.
- [25] S. Talebiesfandarani *et al.*, “Microwave vegetation index from multi-angular observations and its application in vegetation properties retrieval: Theoretical modelling,” *Remote Sens.*, vol. 11, no. 6, pp. 1–20, 2019.

**Lee Ju Hyoung** received the Ph.D. degree in environmental engineering from Politecnico di Milano, Milan, Italy, in 2014.

Focusing on satellite-retrieved soil moisture and satellite data assimilation, she has participated in several international researches including African Monsoon Multidisciplinary Analyses (AMMA) and Tibetan Plateau Experiment under World Meteorological Organization (WMO). As a Principal Investigator, she also has developed an inversion of spaceborne Synthetic Aperture Radar (SAR), Soil Moisture and Ocean Salinity (SMOS), and SMAP microwave data into geophysical and biophysical parameters, their fractal geometry, and stochastic bias correction with the analysis of chaotic behavior. She also serves nonexpert audiences with the stories of how cosmic intelligence such as quantum model, self-organization, randomness, or uncertainty principle helps out our daily lives.